Available online at www.sciencedirect.com
ScienceDirect
Journal of Molecular Catalysis A: Chemical 283 (2008) 158–165
JOURNAL OF MOLECULAR CATALYSIS A: CHEMICAL
www.elsevier.com/locate/molcata

Characterization of Na^+-β-zeolite supported Pd and PdAg bimetallic catalysts using EXAFS, TEM and flow reactor

Wei Huang, Raul F. Lobo, Jingguang G. Chen *

Department of Chemical Engineering, Center for Catalytic Science and Technology (CCST), University of Delaware, Newark, DE 19716, USA

Received 4 July 2007; accepted 5 December 2007
Available online 20 February 2008

Abstract

Flow reactor studies of the selective hydrogenation of acetylene in the presence of ethylene have been performed on Na^+ exchanged β-zeolite supported Pd, Ag and PdAg catalysts, as an extension of our previous batch reactor studies [W. Huang, J.R. McCormick, R.F. Lobo, J.G. Chen, J. Catal. 246 (2007) 40–51]. Results from flow reactor studies show that the PdAg/Na^+-β-zeolite bimetallic catalyst has lower activity than Pd/Na^+-β-zeolite monometallic catalyst, while Ag/Na^+-β-zeolite does not show any activity for acetylene hydrogenation. However, the selectivity for the PdAg bimetallic catalyst is much higher than that for either the Pd catalyst or Ag catalyst. The selectivity to byproduct (ethane) is greatly inhibited on the PdAg bimetallic catalyst as well. The results from the current flow reactor studies confirmed the pervious results from batch reactor studies [W. Huang, J.R. McCormick, R.F. Lobo, J.G. Chen, J. Catal. 246 (2007) 40–51]. In addition, we used transmission electron microscope (TEM), extended X-ray absorption fine structure (EXAFS), and FTIR of CO adsorption to confirm the formation of Pd–Ag bimetallic alloy in the PdAg/Na^+-β-zeolite catalyst.

Keywords: Selective hydrogenation; Acetylene; Ethylene; Pd; Pd–Ag; Bimetallic catalysts; Na^+-β-zeolite; Flow reactor; EXAFS; CO adsorption; TEM

1. Introduction

Selective hydrogenation of acetylene to ethylene is a very important industrial purification process for removing trace amount of acetylene from ethylene [2–5]. Currently, supported Pd catalyst is the commercial catalyst for this purification process [6–8]. However, supported Pd catalyst has poor selectivity at high conversion. Therefore, the addition of a second metal has been attracting considerable attention to enhance the selective hydrogenation of acetylene [5,9–13]. Ag has been reported as a selectivity promoter for the hydrogenation of acetylene into ethylene [9,10,14–16]. In addition to metal active sites, the supports also play an important role. Several reports have demonstrated that porous supports, such as pumice [17] and zeolites [18,19], show better activity, selectivity and stability than traditional Al_2O_3 and SiO_2 supports. Our previous studies [1] also showed that cation exchanged zeolite can selectively adsorb acetylene over ethylene, leading to an increase in the local concentration of acetylene and consequently the hydrogenation selectivity.

Results from our batch reactor studies [1] also showed that PdAg bimetallic catalysts have higher selectivity but lower activity than monometallic Pd catalyst on either γ-Al_2O_3 support or ion-exchanged β-zeolite support. In summary, fitting of the batch reactor experiments indicates that the rate constant of acetylene hydrogenation on PdAg bimetallic catalyst is smaller than that on Pd monometallic catalyst, while the selectivity for acetylene hydrogenation on PdAg is higher than Pd. In the current paper, we conducted flow reactor studies to directly compare PdAg bimetallic catalysts with their parent metals on Na^+-β-zeolite support to confirm previous batch reactor results. Furthermore, we also characterized the materials using transmission electron microscope (TEM), extended X-ray absorption fine structure (EXAFS), and FTIR of CO adsorption, to confirm the formation of bimetallic particles on the Na^+-β-zeolite support.

* Corresponding author. Tel.: +1 302 831 0642; fax: +1 302 831 2085.
E-mail address: jgchen@udel.edu (J.G. Chen).

1381-1169/$ – see front matter © 2008 Elsevier B.V. All rights reserved.
doi:10.1016/j.molcata.2007.12.017

2. Experiment

2.1. Catalyst preparation

Supported catalysts were synthesized using the incipient wetness method as described previously [1]. Prior to metal addition, the β-zeolite (SiO_2:Al_2O_3 = 25, Zeolyst Company, CP814E) was Na^+-exchanged using two treatments of 500 mL, 0.01 M $NaNO_3$ followed by rinsing in DI water and drying at 383 K. The compositions of the synthesized catalysts are as follows: 1.3 wt% Pd/Na^+-β-zeolite, 1.3 wt% Ag/Na^+-β-zeolite and 1.3 wt% Pd–1.3 wt% Ag/Na^+-β-zeolite

2.2. Transmission electron microscopy (TEM) characterization

TEM analyses were performed on spent catalysts from flow reactor studies using a JEOL 2010F equipped with a Schottky field emission gun operated at 200 keV, with an ultra-high resolution pole piece providing a point resolution of 1.9 Å. Energy dispersive X-ray spectroscopy (EDS) provided single-particle elemental analysis using an EDAX Phoenix X-ray spectrometer with a resolution of 134 eV over a 40 keV range. All TEM samples were prepared by grinding and suspending the spent catalyst in ethanol, sonicating the catalyst solution for 5 min, and applying one to two drops of the sonicated solution to a 200- or 300-mesh lacey Cu grid that was then allowed to dry in air.

2.3. FTIR Spectra of adsorbed CO

Fourier transform infrared (FTIR) spectroscopy of CO adsorption was used to probe the surface properties of the catalysts. A Nicoet-510 FTIR spectrometer equipped with a MCT-A (mercury cadmium telluride) detector was used for the CO adsorption experiments. The experiments were performed using a stainless steel IR cell with BaF_2 windows, which allowed in situ reduction of samples and spectroscopic measurements of surface species as described previously [20]. Powder catalyst samples of ∼22 mg were pressed onto a square tungsten mesh. A K-type thermocouple was spot-welded on the mesh to monitor the temperature. To remove water and other impurities, the IR cell was evacuated to a pressure below 10^{-6} Torr at room temperature over night. The catalysts were then reduced at 723 K in 30 Torr hydrogen for 30 min. The ramping rate was 14 K/min from room temperature to 723 K. The cell was then evacuated and a high temperature flash (723 K) was performed to remove any surface species generated during the reduction period. The reduction cycle was repeated three times before performing CO adsorption experiments. After the catalysts were reduced, 1 Torr of CO was introduced into the IR cell for 10 min at room temperature. Surface spectra were then recorded after each of the following procedures: pumping out for 5 min at room temperature, after annealing to 373 K for 30 s and pumping out for 5 min, and after annealing to 423 K for 30 s and pumping out for 5 min. Due to the dipole–dipole interactions of CO with zeolite cations that often lead to the adsorption of CO on zeolites at room temperature [21,22], the spectra taken after annealing to 373 K or 423 K reveal the most useful information about the adsorption of CO on the metal sites.

2.4. Extended X-ray absorption fine structure (EXAFS)

Extended X-ray absorption fine structure technique was used to further confirm the formation of bimetallic particles on Na^+-β-zeolite support. The EXAFS experiments using the Ag (25514 eV) and Pd (24350 eV) K-edges were conducted in the National Synchrotron Light Source at Brookhaven National Laboratory using beamline X-18B. Measurements were carried out in the transmission mode for the Pd K-edge and fluorescence mode for the Ag K-edge at room temperature. A Si(1 1 1) double crystal monochromator was used for the measurements. The energy of the X-ray absorption spectra was calibrated using reference Pd and Ag foils.

The samples for the EXAFS measurements were pressed into a thin pellet with a diameter of 13 mm and a thickness of ∼0.1 mm. The samples were placed in a sealed Kapton cell and reduced under a 5% H_2 in He for 60 min at 723 K using a ramping rate of 14 K/min. Following reduction, the samples were cooled to room temperature in the reduction environment prior to the EXAFS measurement. The EXAFS measurements were performed in the 5% H_2 environment.

2.5. Flow reactor studies

The catalytic activity, selectivity to ethylene, and selectivity to ethane were evaluated using a fixed bed flow reactor. Prior to reaction, the catalysts were reduced in a 50% H_2 in He at 723 K for 60 min. The ramping rate was 14 K/min and the temperature was monitored by a K-type thermocouple outside the quartz reactor. The composition of the gas-phase reactant was a mixture of 2.5% C_2H_2, 2.5% C_2H_4 and 10% H_2 balanced with He. The total flow rate was 220 sccm. An online Gas Chromatograph (GC) (HP 5890) equipped with FID was used to analyze the reaction products. The capillary column was a GS-Carbon PLOT column (Agilent) and the sample gas was analyzed at a constant temperature of 343 K. The reaction temperature was controlled by a water bath. Calibration was completed using a certified gas of 1000 ppm C_2H_2, 1000 ppm C_2H_4 and 1000 ppm C_2H_6 balanced with He. To compare the catalyst selectivity at comparable conversion, 15 mg Pd/Na^+-β-zeolite catalysts balanced with 35 mg quartz chips was used to compare with 50 mg PdAg/Na^+-β-zeolite catalysts.

3. Results and discussion

3.1. TEM measurements

TEM was used to characterize the particle size and composition of the spent catalysts from the flow reactor. Images of the Pd/Na^+-β-zeolite, PdAg/Na^+-β-zeolite and Ag/Na^+-β-zeolite are shown in Fig. 1. For the Pd/Na^+-β-zeolite catalyst, the Pd particles are well distributed between 1 nm and 3 nm with few agglomerates ranging between 5 nm and 10 nm. The

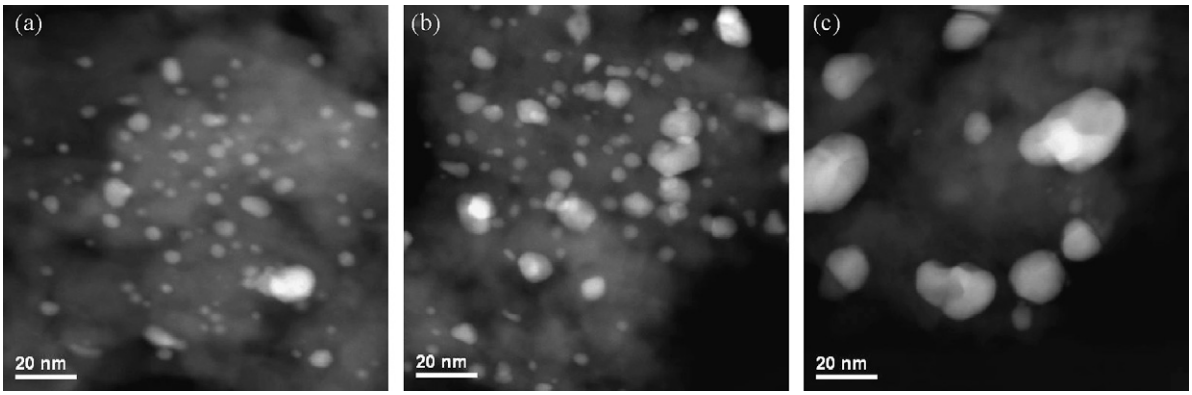

Fig. 1. TEM of spent: (a) Pd/Na^+-β-zeolite (b) PdAg/Na^+-β-zeolite and (c) Ag/Na^+-β-zeolite catalyst samples.

particle size for the PdAg/Na^+-β-zeolite sample is larger than Pd/Na^+-β-zeolite with more agglomerate formation. For the Ag/K^+-β-zeolite catalyst, particles were polydispersed and ranged between 3 nm and 30 nm. The Pd dispersion of the Pd/Na^+-β-zeolite is 23.1% and that of the PdAg/Na^+-β-zeolite is 20.9% as determined using CO-chemisorption measurement [1].

Energy dispersive X-ray spectroscopy (XEDS) was used to analyze the composition of the particles in the PdAg/Na^+-β-zeolite catalyst. The results from several nanoparticles are shown in Fig. 2. It is evident that the characteristic K-edge peaks for both Pd and Ag were observed in the same particle. Particles with only Ag or Pd were not found, indicating that the Pd and Ag were well mixed in the Na^+-β-zeolite support and that the bimetallic particles were formed. The varying intensity ratios of the Pd K-edge and Ag K-edge in different particles indicate that the bimetallic content is slightly different for various particles on the Na^+-β-zeolite support.

3.2. FTIR of adsorbed CO

CO adsorption using FTIR was performed to probe the surface composition of the catalysts. Fig. 3 shows the IR spectra

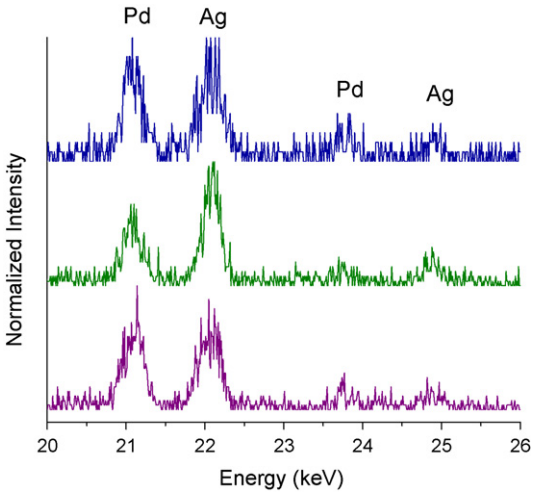

Fig. 2. XEDS of selected particles using HAADF images of PdAg/Na^+-β-zeolite.

of adsorbed CO on Na^+-β-zeolite, Pd/Na^+-β-zeolite, Ag/Na^+-β-zeolite and PdAg/Na^+-β-zeolite catalysts. After exposing the catalysts to 1 Torr CO for 10 min, followed by evacuation for 5 min, the presence of physisorbed CO on the zeolite substrates is detected at room temperature. After annealing the sample to 373 K or 423 K and pumping out for 5 min, the physisorbed CO desorbs and only chemisorbed CO is present on the catalyst surface, as shown in Fig. 3b and c. There is little chemisorbed CO present on either Na^+-β-zeolite or Ag/Na^+-β-zeolite after annealing to 373 K or 423 K.

Two main vibration modes are observed on Pd/Na^+-β-zeolite at 2080 cm^{-1} and 1927 cm^{-1}, which are generally attributed to linear and bridge-bonded CO, respectively [23–25]. Only linear CO is present on PdAg/Na^+-β-zeolite, with the peak centered at 2048 cm^{-1}. As reported previously [26], CO molecule can only form chemical bonds with Pd atoms when exposing a PdAg alloy to CO. The disappearance of the bridge-bond CO on PdAg/Na^+-β-zeolite indicates that the Pd atoms are most likely isolated by Ag atoms on the catalyst surface, suggesting that the bimetallic alloy of PdAg is formed on the catalyst surface.

3.3. EXAFS measurements

EXAFS measurements were performed on PdAg/Na^+-β-zeolite catalyst to verify the formation of bimetallic particles on the Na^+-β-zeolite. For comparison, the EXAFS measurements were performed on the Pd/Na^+-β-zeolite as well. The fitting for Pd K-edge of Pd/Na^+-β-zeolite is shown in Fig. 4 and the parameters from EXAFS fitting analysis and quality of fits are list in Table 1. The fitted Pd–Pd distance is 2.735 ± 0.003 Å, which is slightly smaller than the bulk Pd–Pd first nearest number distance (2.751 Å). This is due to the particle size effect on the interatomic distance. The coordination number of Pd–Pd is 10.3 ± 0.6, which is consistent with the presence of some larger Pd nanoparticles observed in TEM measurement.

The measurement of coordination numbers of heterometallic bonds in Pd–Ag system is not meaningful because the Z-contrast between Pd and Ag is too small. To solve the problem, the EXAFS spectra were fitted by assuming only Pd–Pd and Ag–Ag contribution for each element. The results of fitting are shown in Fig. 5 and Table 1. The first nearest neighbor distances of Pd–Pd and Ag–Ag in bulk metals are 2.751 Å and 2.889 Å,

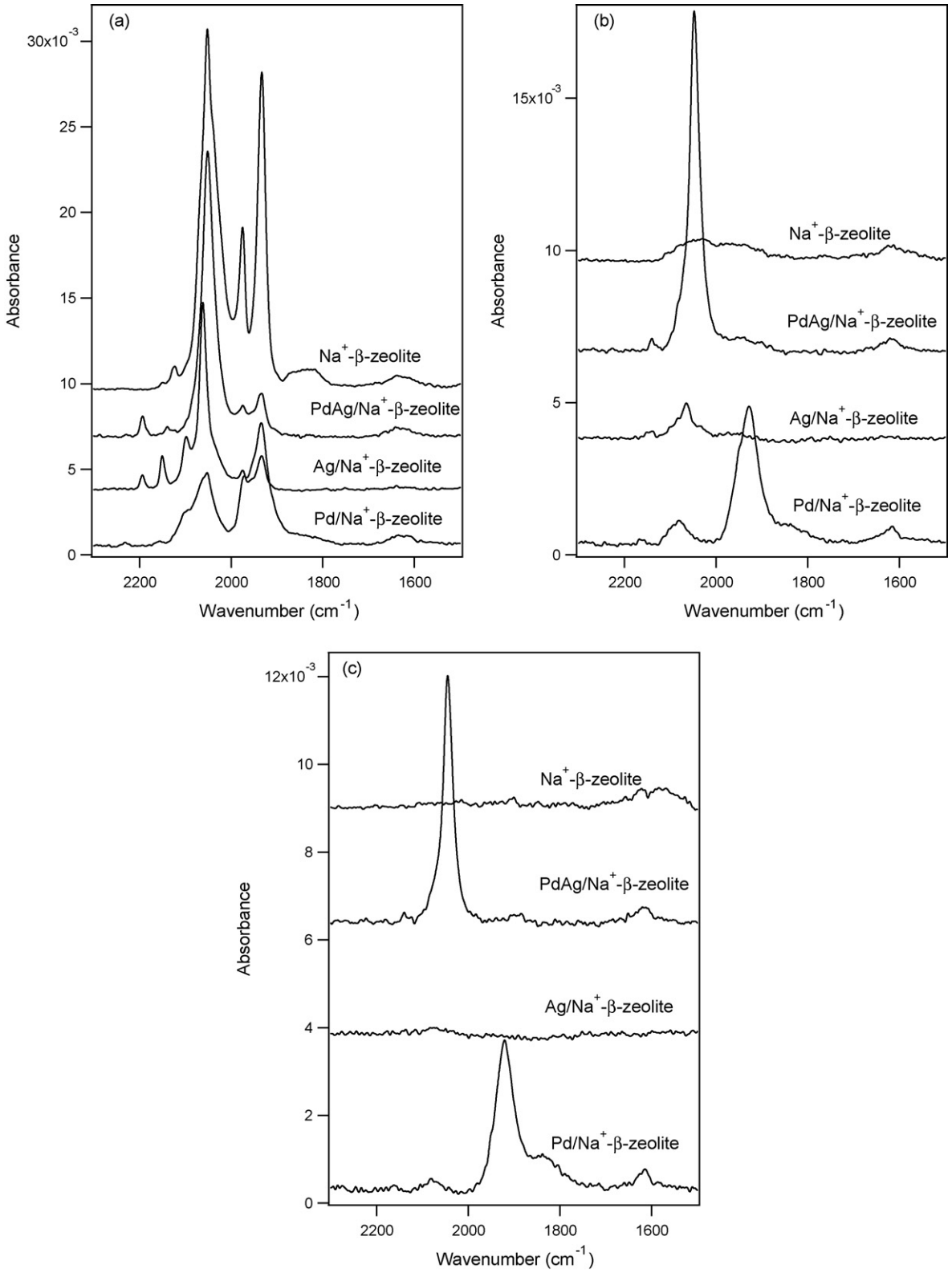

Fig. 3. FTIR spectra of CO adsorption on Na^+-β-zeolite, Pd/Na^+-β-zeolite, PdAg/Na^+-β-zeolite and Ag/Na^+-β-zeolite after: (a) after pumping out for 5 min at room temperature, (b) after annealing to 373 K for 30 s and pumping out for 5 min, and (c) after annealing to 423 K for 30 s and pumping out for 5 min.

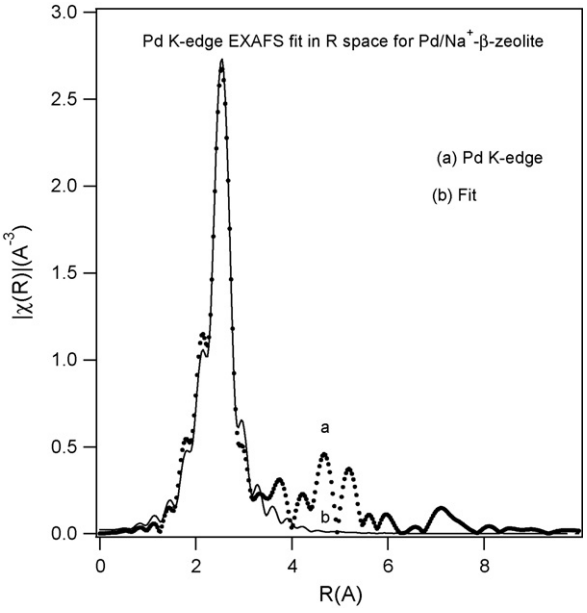

Fig. 4. Pd K-edge of Pd/Na^+-β-zeolite from EXAFS fitting.

respectively. In principle, the first nearest neighbor distance should be similar or slightly smaller than in the bulk if the Pd and Ag segregate to form monometallic nanoparticles. In the case of alloying, the nearest neighbor distance should be an intermediate value between the two monometallic distances. As shown in Table 1, for $PdAg/Na^+$-β-zeolite, the Pd–Pd distance increase to 2.812 ± 0.003 Å and the Ag–Ag distance decrease to 2.822 ± 0.004 Å, which indicate that the Pd and Ag form bimetallic alloy on the Na^+-β-zeolite support. The combined coordination number for Pd edge and Ag edge is 10.7 ± 0.6 and 10.4 ± 0.7, respectively. It is consistent with the sizes of nanoparticles observed in TEM measurements (Fig. 1) based on previous correlations of particle sizes with coordination numbers [27].

Table 1
Parameters derived from the EXAFS analysis of Pd/Na^+-β-zeolite and $PdAg/Na^+$-β-zeolite catalysts

	Pd/Na^+-β-zeolite	$PdAg/Na^+$-β-zeolite
N(Pd–Pd)	10.3 ± 0.6	10.7 ± 0.6
N(Ag–Ag)		10.4 ± 0.7
R(Pd–Pd) (Å)	2.735 ± 0.003	2.812 ± 0.003
R(Ag–Ag) (Å)		2.822 ± 0.004
σ^2(Pd–Pd) (Å^2)	0.0059 ± 0.0003	0.0076 ± 0.0004
σ^2(Ag–Ag) (Å^2)		0.0086 ± 0.0005

3.4. Flow reactor studies

To corroborate the conclusions from our previous batch reactor studies [1], here we utilize the flow reactor system to study the acetylene hydrogenation in the presence of ethylene. The definitions of conversion ($X_{C_2H_2}$), selectivity ($S_{C_2H_6}$) to byproduct (C_2H_6), and selectivity to ethylene ($S_{C_2H_4}$) are adopted from the literature and are defined as

$$X_{C_2H_2} = \frac{C_2H_{2,\text{feed}} - C_2H_{2,\text{final}}}{C_2H_{2,\text{feed}}} \quad (1)$$

$$S_{C_2H_6} = \frac{C_2H_{6,\text{final}}}{C_2H_{2,\text{feed}} - C_2H_{2,\text{final}}} \quad (2)$$

$$S_{C_2H_4} = \frac{C_2H_{4,\text{final}} - C_2H_{4,\text{feed}}}{C_2H_{2,\text{feed}} - C_2H_{2,\text{final}}} \quad (3)$$

To compare the catalysts at comparable conversions, 15 mg Pd/Na^+-β-zeolite catalyst was used as compared to 50 mg $PdAg/Na^+$-β-zeolite catalyst. As shown in Fig. 6, the C_2H_4 selectivity on $PdAg/Na^+$-β-zeolite was nearly three times higher than on Pd/Na^+-β-zeolite at a similar conversion at 333 K. On the other hand, the C_2H_6 selectivity on $PdAg/Na^+$-β-zeolite, which was the undesirable byproduct, was only 1/3 of that on Pd/Na^+-β-zeolite. The Ag/Na^+-β-zeolite did not show any activity for

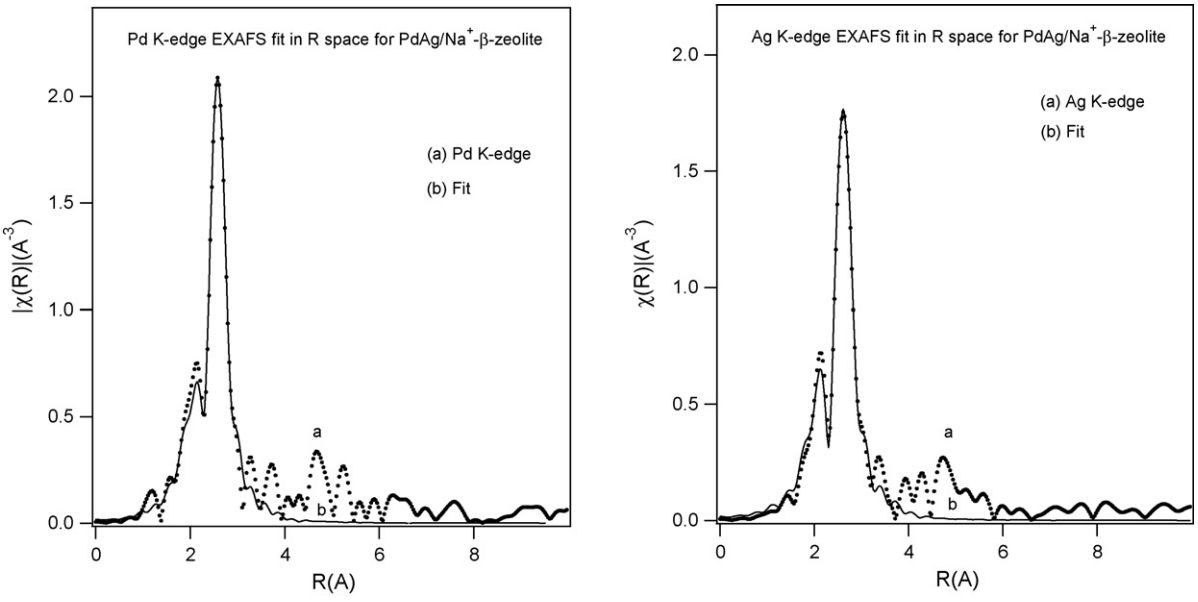

Fig. 5. Pd K-edge and Ag K-edge of $PdAg/Na^+$-β-zeolite catalysts from EXAFS fitting.

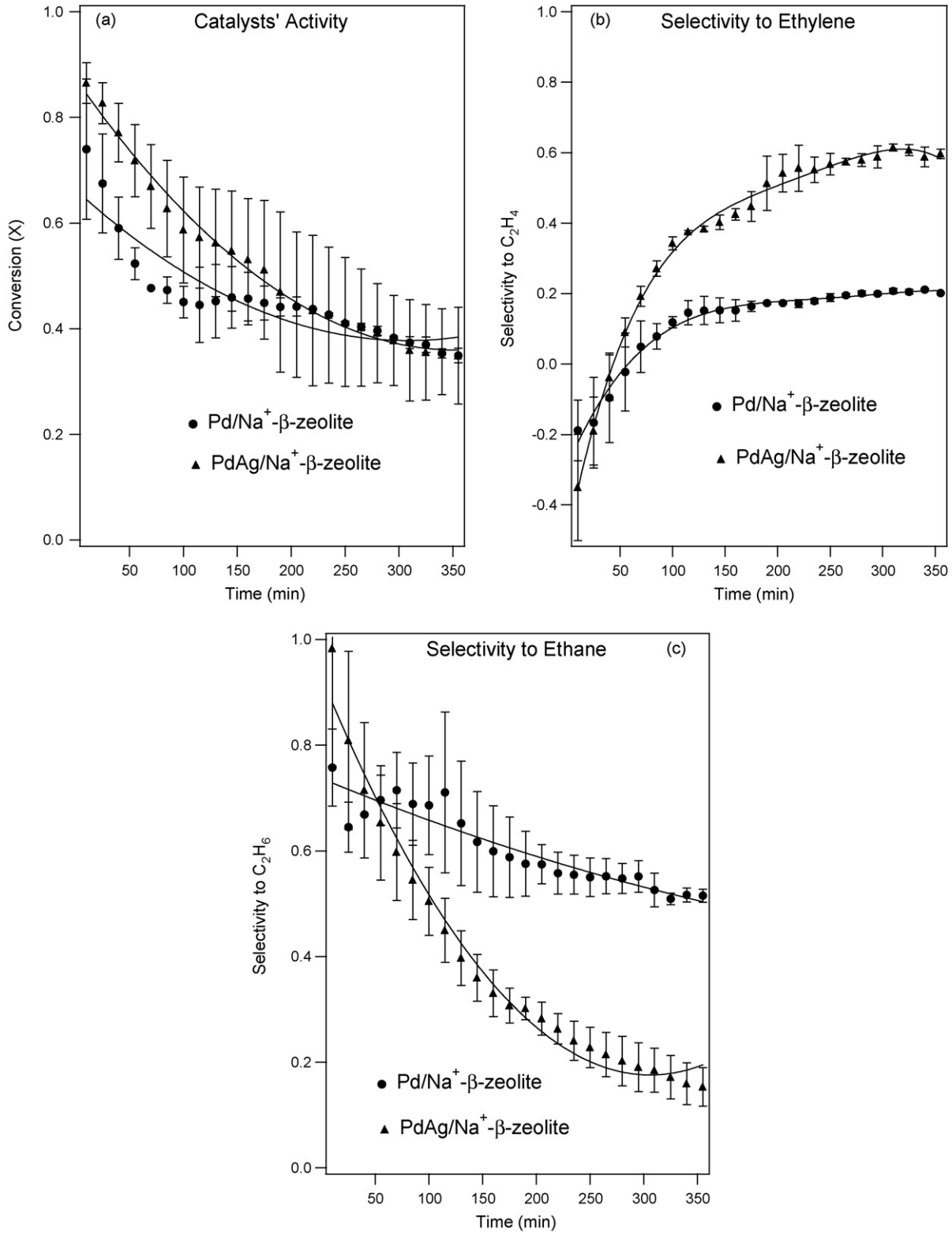

Fig. 6. (a) Activity of acetylene hydrogenation, (b) C_2H_4 selectivity and (c) selectivity of byproduct C_2H_6 of Pd/Na^+-β-zeolite and PdAg/Na^+-β-zeolite. Experimental conditions: C_2H_2:C_2H_4:H_2 = 1:1:4, reaction temperature: 333 K, catalysts amount: 50 mg for PdAg/Na^+-β-zeolite and 15 mg for Pd/Na^+-β-zeolite mixed with 35 mg quartz chips.

the selective hydrogenation of acetylene in ethylene (Figure not shown). This is consistent with the batch reactor results that PdAg/Na^+-β-zeolite shows lower activity but higher selectivity than Pd/Na^+-β-zeolite.

The apparent activation barrier of acetylene hydrogenation on Pd/Na^+-β-zeolite and PdAg/Na^+-β-zeolite was also measured. The Arrhenius plot is shown in Fig. 7 and the estimated apparent activation barrier on Pd/Na^+-β-zeolite and PdAg/Na^+-β-zeolite

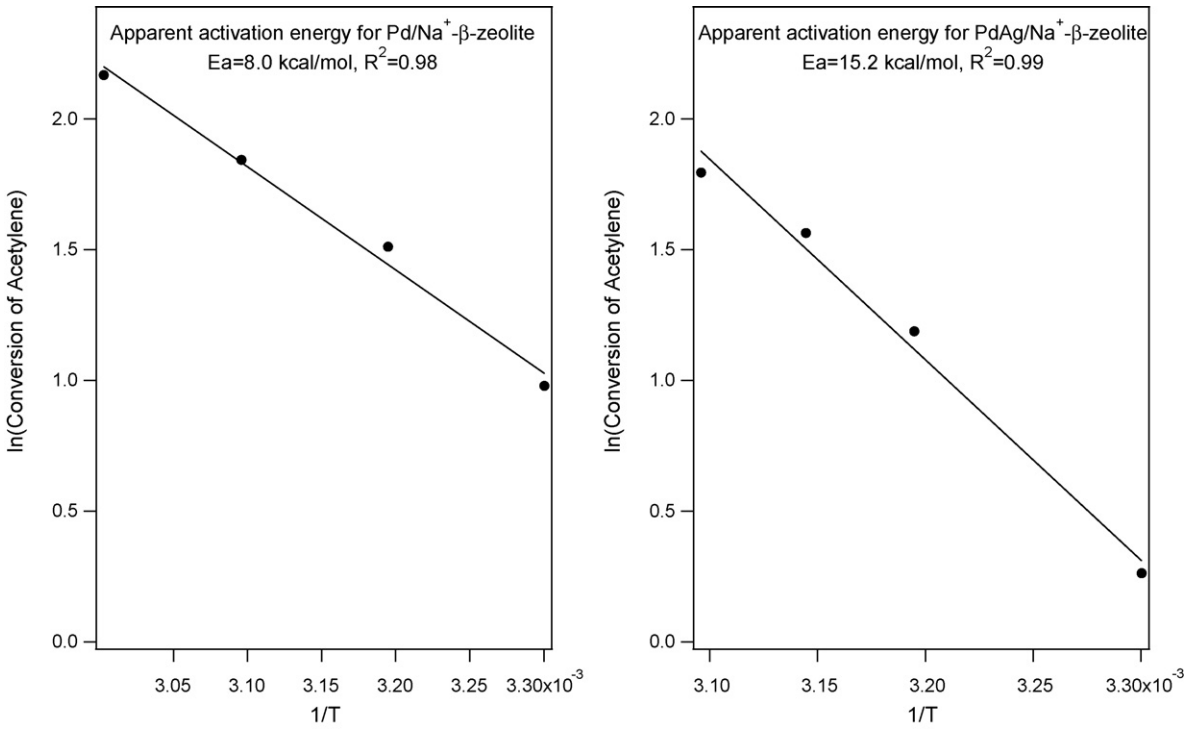

Fig. 7. Estimation of apparent activation energy of Pd/Na^+-β-zeolite and PdAg/Na^+-β-zeolite for acetylene conversion in acetylene–ethylene mixture (C_2H_2:C_2H_4:H_2 = 1:1:4).

is 8.0 kcal/mol and 15.2 kcal/mol, respectively. The activation energy of acetylene hydrogenation varies with different supports and experimental conditions. Bodnariuk and coworkers [28] reported values between 15 kcal/mol and 16 kcal/mol on two types of Al_2O_3 supported Pd under industrial conditions. Weiss and coworkers[18] have found that the activation energy was about 13–14 kcal/g mol on several zeolite supported Pd catalysts. Duca et al. [29] compared Pd catalysts supported on pumice and alumina and reported activation energy values ranging from 8.6 kcal/mol to 25.2 kcal/mol. The activation energy on PdAg/α-Al_2O_3 was also reported by Bond et al. [30] to be 20.1 ± 0.5 kcal/mol between 293 K and 353 K. The activation barriers of acetylene hydrogenation on Na^+-β-zeolite supported Pd and PdAg catalysts are slightly smaller than the literature reports on other substrates. However, the trend is consistent with the rate constant of acetylene hydrogenation on Pd/Na^+-β-zeolite and PdAg/Na^+-β-zeolite derived from batch reactor studies [1].

4. Conclusions

We found that alloying Pd with Ag reduced the acetylene hydrogenation activity but increased the selectivity. The apparent activation energy of acetylene hydrogenation on Pd/Na^+-β-zeolite and PdAg/Na^+-β-zeolite were estimated to be 8 kcal/mol and 15.2 kcal/mol. In addition, the formation of PdAg bimetallic particles on the Na^+-β-zeolite support was confirmed by TEM, EXAFS, and CO adsorption using FTIR spectroscopy.

Acknowledgements

We acknowledge financial support from the US Department of Energy, Office of Sciences, Division of Chemical Sciences (grant FG02-03ER15468). We also acknowledge Mr. W. Pyrz, Dr. C. Ni and the Keck Microscopy facility for access and assistance in electron microscopy. We thank Dr. Frenkel, Dr. Marinkovic and DOE grant FG02-05ER15688 for help with EXAFS measurements and analysis.

References

[1] W. Huang, J.R. McCormick, R.F. Lobo, J.G. Chen, J. Catal. 246 (2007) 40–51.
[2] J.H. Kang, E.W. Shin, W.J. Kim, J.D. Park, S.H. Moon, Catal. Today 63 (2000) 183–188.
[3] N.S. Schbib, M.A. Garcia, C.E. Gigola, A.F. Errazu, Ind. Eng. Chem. Res. 35 (1996) 1496–1505.
[4] W.J. Kim, J.H. Kang, I.Y. Ahn, S.H. Moon, Appl. Catal. A: Gen. 268 (2004) 77–82.
[5] P. Praserthdam, S. Phatanasri, J. Meksikarin, Catal. Today 63 (2000) 209–213.
[6] H. Molero, B.F. Bartlett, W.T. Tysoe, J. Catal. 181 (1999) 49–56.
[7] A. Sarkany, A. Beck, A. Horvath, Z. Revay, L. Guczi, Appl. Catal. A: Gen. 253 (2003) 283–292.
[8] B.M. Choudary, M.L. Kantam, N.M. Reddy, K.K. Rao, Y. Haritha, V. Bhaskar, F. Figueras, A. Tuel, Appl. Catal. A: Gen. 181 (1999) 139–144.
[9] P. Praserthdam, B. Ngamsom, N. Bogdanchikova, S. Phatanasri, M. Pramotthana, Appl. Catal. A: Gen. 230 (2002) 41–51.
[10] R.N. Lamb, B. Ngamsom, D.L. Trimm, B. Gong, P.L. Silveston, P. Praserthdam, Appl. Catal. A: Gen. 268 (2004) 43–50.
[11] C. Visser, J.G. Zuidwijk, V. Ponec, J. Catal. 35 (1974) 407–416.

[12] S. Leviness, V. Nair, A.H. Weiss, Z. Schay, L. Guczi, J. Mol. Catal. 25 (1984) 131–140.
[13] A. Sarkany, A. Horvath, A. Beck, Appl. Catal. A: Gen. 229 (2002) 117–125.
[14] P.A. Sheth, M. Neurock, C.M. Smith, J. Phys. Chem. B 109 (2005) 12449–12466.
[15] H. Zea, K. Lester, A.K. Datye, E. Rightor, R. Gulotty, W. Waterman, M. Smith, Appl. Catal. A: Gen. 282 (2005) 237–245.
[16] Y.M. Jin, et al., J. Catal. 203 (2001) 292–306.
[17] D. Duca, F. Frusteri, A. Parmaliana, G. Deganello, Appl. Catal. A: Gen.** 146 (1996) 269–284.
[18] W.L. Kranich, A.H. Weiss, Z. Schay, L. Guczi, Appl. Catal. 13 (1985) 257–267.
[19] D.R. Corbin, L. Abrams, C. Bonifaz, J. Catal. 115 (1989) 420–429.
[20] P. Basu, T.H. Ballinger, J.T. Yates, Rev. Sci. Instrum. 59 (1988) 1321–1327.
[21] F.J. Maldonado, T. Becue, J.M. Silva, M.F. Ribeiro, P. Massiani, M. Kermarec, J. Catal. 195 (2000) 342–351.
[22] T. Becue, F.J. Maldonado-Hodar, A.P. Antunes, J.M. Silva, M.F. Ribeiro, P. Massiani, M. Kermarec, J. Catal. 181 (1999) 244–255.
[23] A. Elhamdaoui, G. Bergeret, J. Massardier, M. Primet, A. Renouprez, J. Catal. 148 (1994) 47–55.
[24] Y. Somanoto, W.M. Sachtler, J. Catal. 32 (1974) 315–324.
[25] M.S. Li, J.Y. Shen, Mater. Chem. Phys. 68 (2001) 204–209.
[26] B. Heinrichs, F. Noville, J.P. Schoebrechts, J.P. Pirard, J. Catal. 192 (2000) 108–118.
[27] A.I. Frenkel, C.W. Hills, R.G. Nuzzo, J. Phys. Chem. B 105 (2001) 12689–12703.
[28] C.E. Gigola, H.R. Aduriz, P. Bodnariuk, Appl. Catal. 27 (1986) 133–144.
[29] D. Duca, F. Arena, A. Parmaliana, G. Deganello, Appl. Catal. A: Gen. 172 (1998) 207–216.
[30] G.C. Bond, D.A. Dowden, N. Mackenzie, Trans. Faraday Soc. 54 (1958) 1537–1546.